ICAS 2020 SHANG HAI
International Council of the Aeronautical Sciences
32nd Congress of the International Council of the Aeronautical Sciences
September 6-10, 2021
Pudong Shangri-La, Shanghai, China

The Development of Algorithms for EMA Fault Early Detection System

Sergey Bazhenov[1], Alexey Skryabin[1], Georgy Veresnikov[2]

[1]Central Aerohydrodynamic Institute of Russia
[2]Institute of Control Science of Russian Academy of Science

Abstract

The paper deals with the problem of early detection algorithm construction to identify failures of aircraft electromechanical actuator (EMA). A scheme for processing EMA operation data using data mining methods is proposed. Methods of feature selection are described, which are used to reduce the dimension of the controlled parameters vector. The computational experiments results based on the data obtained using the mathematical model of the UAV control surface EMA are presented.

Keywords: electromechanical actuator, early failure detection, neural networks

1. Introduction

With the development of electric aircraft (A/C) creation technologies, the relevance of the detecting control surface EMA failures algorithms development increases, the effectiveness of which significantly depends on flight safety [1-3]. The need to improve the A/C flight safety indicators and reduce service costs determine the relevance of the development and implementation of EMA health usage monitoring systems (HUMS). Studies [4-7] of EMA HUMS conducted by leading aviation design bureaus and research organizations in this area have shown the effectiveness of the integration of data mining methods (DM) and the method of comparing the functioning of full-scale system signals with a mathematical model for monitoring the EMA technical state. The DM methods usage makes it possible to solve the problem of assessing the EMA technical state when there is no sufficient amount of data to accept statistical hypotheses with the required level of confidence and detailed mathematical models of EMA, allowing to take into account all kinds of internal and external factors. As part of solving the problem of developing EMA failure detection algorithm associated with a change in the dissipative losses, the article presents:

– EMA operation data processing scheme using neural networks;

– feature selection algorithms description to improve the efficiency of using neural networks in the problem EMA faulures detection;

– the study results of the proposed data processing scheme on the data obtained using the UAV EMA mathematical model.

2. Data processing scheme

A scheme for processing data on the operation of EMF is proposed (Figure 1), the result of which is an algorithm for detecting EMF malfunctions.

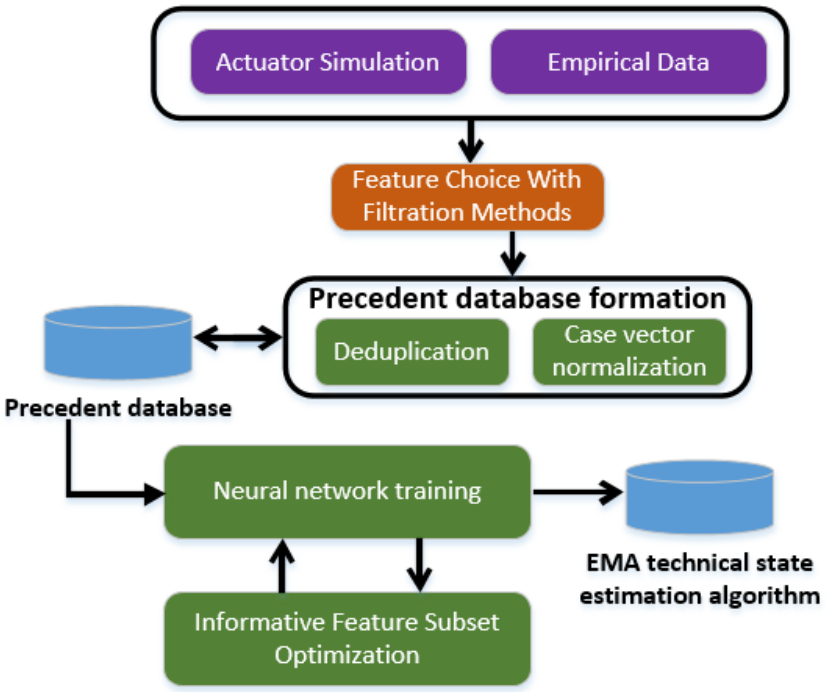

Figure 1 – Data processing scheme.

One of the ways to determine degradations developing in an EMA before failure is to monitor and analyze dissipative energy losses. The problem of algorithm construction for detecting EMA faults associated with a change in dissipative losses, within the framework of the proposed scheme, is formalized as a classification problem into two classes. Based on data on the EMA operation $\{(\bar{x}_1, \bar{y}_1), \dots, (\bar{x}_k, \bar{y}_k)\}$, $\bar{x}_i \in X$, $\bar{y}_i \in Y$, i=1..*k*, it is necessary to build an algorithm for detecting EMA faults $\Phi: X \to Y$, where X – a set of attribute values - monitored and control EMA parameters, Y – a set consisting of class labels reflecting the EMA technical condition.

The initial data on the EMA operation are formed on the basis of its mathematical model, which takes into account the influence of the dissipative torque on the EMA controlled parameters. In the future, the data obtained using the EMA simulation are supplemented with statistical data accumulated as a result of A/C flights. As a result of the choice of a method / set of methods for filtering features, an algorithm is formed $\Omega: X \to H$, where H – set of vectors of reduced dimension. Within the framework of the scheme in Figure 1, the Ω algorithm is applied to the set of EMA states $\{(\bar{x}_1, \bar{y}_1), \dots, (\bar{x}_k, \bar{y}_k)\}$, $\bar{x}_i \in X$, $\bar{y}_i \in Y$, i=1..k convert to set $\{(\bar{h}_1, \bar{y}_1), \dots, (\bar{h}_k, \bar{y}_k)\}$, $\bar{h}_i \in H$, $\bar{y}_i \in Y$, i=1..k, which is input information for DM methods.

Before inclusion the set $\{(\bar{h}_1, \bar{y}_1), \dots, (\bar{h}_k, \bar{y}_k)\}$ to precedent database, formed for DM methods application.

1. Searching and excluding vectors $\bar{h}_i$, i=1..k, which contain redundant information. In order to perform this procedure, vector similarity metrics and clustering methods are used to reduce the training sample size.

2. Normalization of the remaining vectors from the set $\{\bar{h}_1, \dots, \bar{h}_k\}$ on a unit interval to eliminate the influence of the digit capacity of numbers on the result of the algorithm Λ, encoding of class labels.

Further, using the DM method chosen by the developer, the patterns search and formalization is performed (an algorithm is constructed $\Lambda: H \to Y$ classification of EMA states based on a set of vectors H), contained in the base of use cases, in integration with a method that optimizes a subset of informative features (wrapper methods), which makes it possible to further reduce the elements number of vector $\bar{h}$ and improve the accuracy of the algorithm Λ. Optimization of informative features subset in the work is performed using direct enumeration to obtain a global extremum or genetic algorithms to obtain an approximate solution. The resulting algorithm Φ is used to assess the EMA state. For this, a vector of monitored parameters values is fed to the input of the neural network, and an assessment of the EMA technical state is formed at the output.

3. Feature filtering

To reduce the dimension of the input parameters vector of the Φ algorithm, a procedure consisting of two stages is used.

Stage 1. Sorting features based on the statistical chi-square test. As a result of this test, the criterion χ^2 is calculated for each feature from the vector of monitored EMA parameters $\overline{x}$ according to the well-known formula [8]. The most informative for solving the classification problem is considered a feature for which χ^2 has a maximum value.

Stage 2. Construction of nonlinear multiple regression models.

At the next stage, to find complex dependencies between the input parameters of the algorithm Λ (elements of vector $\overline{x}$) it is proposed to use nonlinear multiple regression, which allows finding a single analytical expression - an approximating function (usually polynomials are used), over the entire domain of its definition. To apply multiple nonlinear regression, you need to select the basis functions that are included in the multiple regression model:

$$h_i(\overline{x}^{'}) = \sum_{d=1}^{N} a_d B_d\left(\overline{x}^{'}\right),$$

where x_i – dependent feature from vector $\overline{h}$, $B_d(\overline{h}')$ - basis function, a_d – the estimated coefficient of the model, $\overline{x}^{'} = \overline{x} \backslash x_i$, N – number of basis function.

If the number of parameters of the function being approximated is more than one, then the formation of basis functions can be difficult. In this regard, a more efficient approach to constructing a multiple nonlinear regression model is used, which provides for the execution of Algorithm 1.

Algorithm 1.

1. Formation by the EMA developer of a set of elementary functions $b_j(x')$, $x' -$ is an arbitrary feature from the vector $\bar{x}'$, j=1..z, z – is the number of elementary functions.
2. The choice of the way of integrating the functions $b_j(\bar{x}')$ to form the basis functions $B_d(\bar{x}')$.

   For example, let on the basis of the elementary functions $\{b_1(x'), \dots, b_z(x')\}$, selected by the developer, a set is formed:

   $G = \{b_1(x_1), \dots, b_z(x_1), \dots, b_1(x_{k-1}), \dots, b_z(x_{k-1}), 1^0, \dots, m^0\}$,

   where m is the number of elements of the set G used to form one basic function (set by the EMA developer), k-1 – is the number of elements of the vector $\bar{x}'$.

   Then the basis functions $B_d(\bar{x}')$, d=1,..,N, where $N = (k+m-1)!/(m!\,(k-1)!)$, Are products of elements of combinations from the set G with respect to m.
3. Construction of a multiple nonlinear regression model (estimation of the coefficients $a_d, d = 1, \dots, N$).

End of Algorithm 1.

To assess the quality of the found multiple regression model, the standard coefficient of determination R^2 is used which varies from 0 to 1. If R^2 is close to 1 (a specific threshold value is set by the data scientist), then the dependent parameter can be excluded from the subset of vector $\overline{h}$ features used to assess the EMA technical condition.

If the list of features sorted at stage 1 contains features between which there is a high regression relationship (threshold R^2), hen interdependent features with the smallest χ^2 are excluded from this list.

4. EMA mathematical model

Based on the middle-range UAV EMA design characteristics and the results of its experimental studies in the Simulink environment, a mathematical model of the EMA was developed [9]. The EMA consists of a brushless electric motor, a power electronics control unit and a 6-stage spur gear, integrated into one housing, its characteristics are presented in Table 1.

Table 1 – EMA main characteristics.

Nominal torque, Н·м	Stall torque, Н·м	No load rotation speed, °/c	Output stroke, °	Supply voltage, В	Nominal current, А	Mass, кг
3,5	5	100	±60	27	0,85	0,36

The main equation that determines the torque balance acting on the electric motor (Figure 2) is as follows [10]:

$$T_{EM} = T_J + T_{Ext} + T_E + T_D,$$

where $T_{EM} = k_t I_s$ - electromagnetic torque developed on the rotor shaft, obtained from the product of the torque coefficient k_t and stator phase current I_s. The current in the stator winding is determined from Ohm's law for the rotor phase:

$$\frac{dI_s}{dt} = \frac{U_s - R_s I_s - Ubemf}{L_s},$$

where U_s, R_s, L_s – stator phase voltage, resistance and inductance. $Ubemf = k_t \omega$ - back-EMF voltage arising in the stator windings when the rotor rotates at a speed ω.

T_{Ext} – external load (hinge torque); T_E – the torque of elastic deformation of the gearbox, T_D – dissipative torque, which is used to establish different levels of EMA degradation, characterized by energy dissipation. To simulate the dissipative torque in this work, the Coulomb friction model is used (Figure 2). The dissipative torque determined by this method makes it possible to estimate the order of the generalized energy losses due to friction in the no-load condition. A more detailed description of the mechanic dissipative torque model is possible when modeling a two-mass system "electric motor rotor – reducer" and taking into account Karnop friction [11]. Acceleration rate $\dot{\omega}$ determines the inertial torque $T_J = \dot{\omega} J$ rotating units of the joint venture, where $J=J_{rot}+J_{gear}$ moment of inertia of the electric motor rotor and gear.

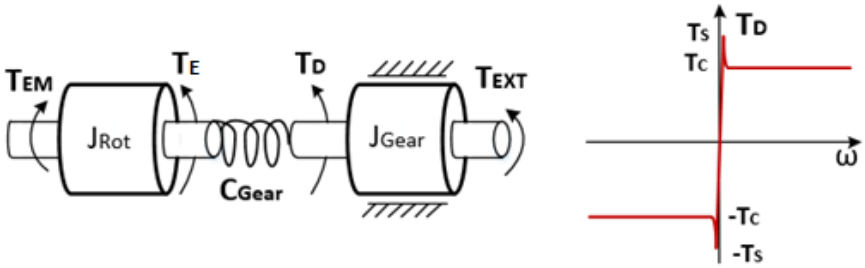

Figure 2 – Kinematic diagram of the EMA mechanics model (left) and the nature of the change in the dissipative moment (Coulomb friction model) (right).

5. Results of computational studies

The EMA operation data for the study of the data processing scheme presented in Figure 1 were obtained using the EMA mathematical model described in the previous section. The simulation used an input signal corresponding to the cyclogram of the UAV takeoff. To form the training and test sample, which contains various options for the EMA technical states, the value of the Coulomb friction Tc was varied (Table 1), the growth of which is due to the development of degradations in the EMA mechanical system. The stiction friction value is taken as Ts = Tc * 1.2.

Table 1 – Splitting data into training and test samples

Couloumb friction Tc, Nm	Sample type	Class
0.225	Training	Normal operation
0.275	Test	Normal operation
0.325	Test	Normal operation
0.375	Test	Normal operation
0.875	Test	Emergency condition
0.925	Test	Emergency condition
0.975	Test	Emergency condition
1.025	Test	Emergency condition

The class that determines the EMA state is specified by a categorical variable (has a non-numerical nature), which is encoded in the class label by binary numbers for the use of neural networks. Accordingly, the output vector $\overline{y}$ (in this case, the output of the neural network) consists of two numerical variables that determine the EMA technical state (Table 3).

Таблица 3 – Numeric encoding of the EMA technical condition class label.

Class serial number	EMA technical condition class	Class label (binary code of EMA technical condition)
1	Normal technical condition	(0,1)
2	Emergency technical condition	(1,0)

It means the principle "winner takes everything" is used, when classes are encoded with the values of binary neurons (each neuron corresponds to one class and the class of technical state is determined by the neuron at the output of which the maximum value is observed). As a result of working out the UAV flight cyclogram for the values of Tc indicated in Table 2, data on the EMA operation were generated, which include the following EMA parameters:

- V1 – input signal (°),
- V2 – rotor rotation (°),
- V3 – output shaft signal (°),
- V4 – supply voltage (V),
- V5 – supply current (A),
- V6 – supply electric power (W),
- V7 – rotor rotation speed (rev/min),
- V8 – rotor shaft torque (Nm),
- V9 – rotor shaft mechanic power (W),
- V10 – output shaft rotation speed (rev/min),
- V11 – output shaft torque (Nm),
- V12 – output shaft mechanic power (W).

As a result, the training and test samples for each class of the EMA technical state contain the values of the parameters V1-V12, recorded during the flight cyclogram processing for 100 s. every 0.01 s. Figures 3-14 show examples of changing the V1-V12 parameters for Tc = 0.225 (training sample, class No. 1).

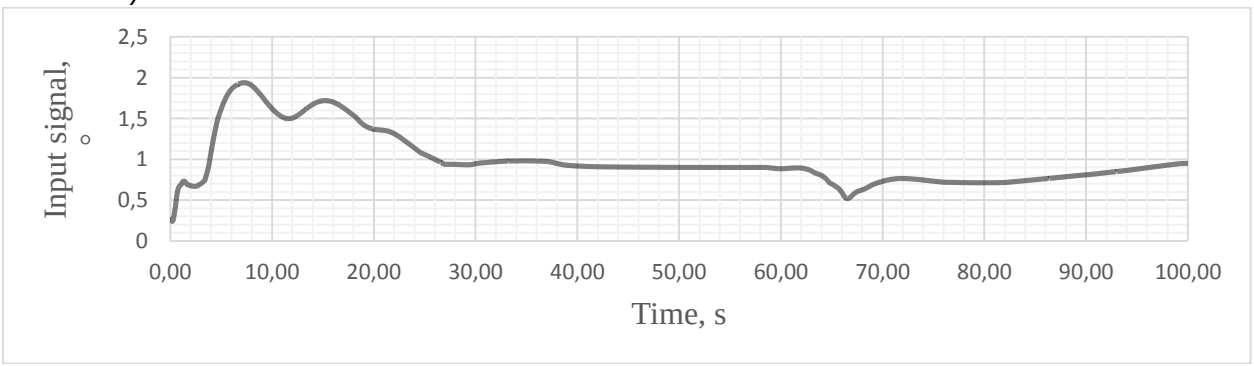

Figure 3 – An example of changing an input variable V1

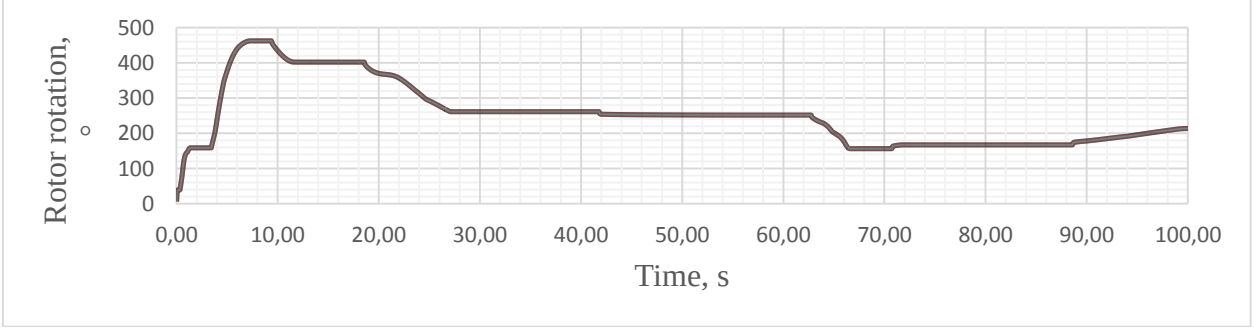

Figure 4 – An example of changing an input variable V2

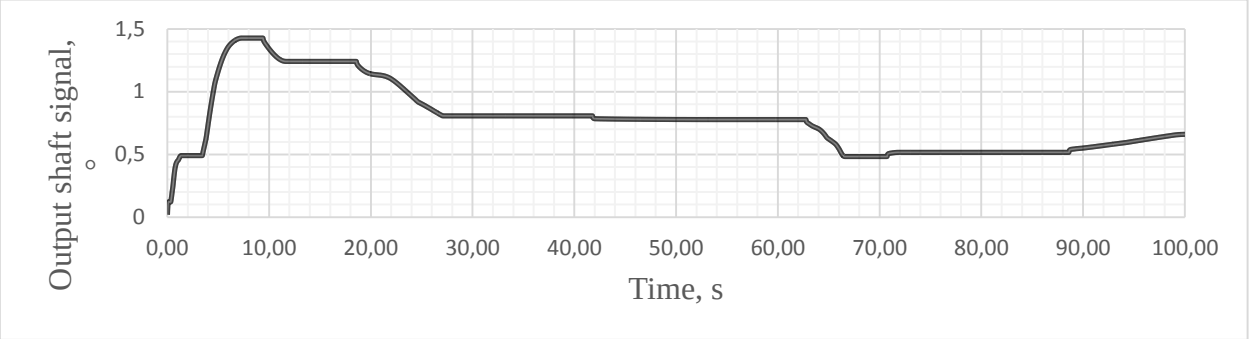

Figure 5 – An example of changing an input variable V3

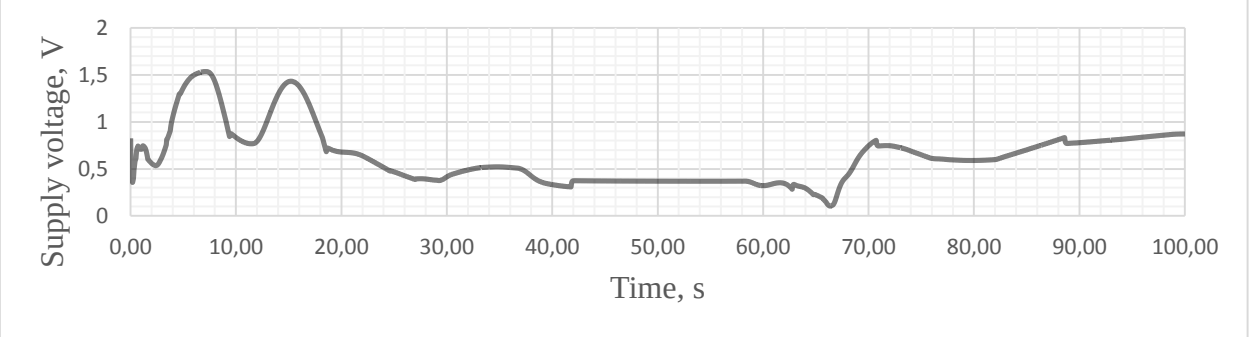

Figure 6 – An example of changing an input variable V4

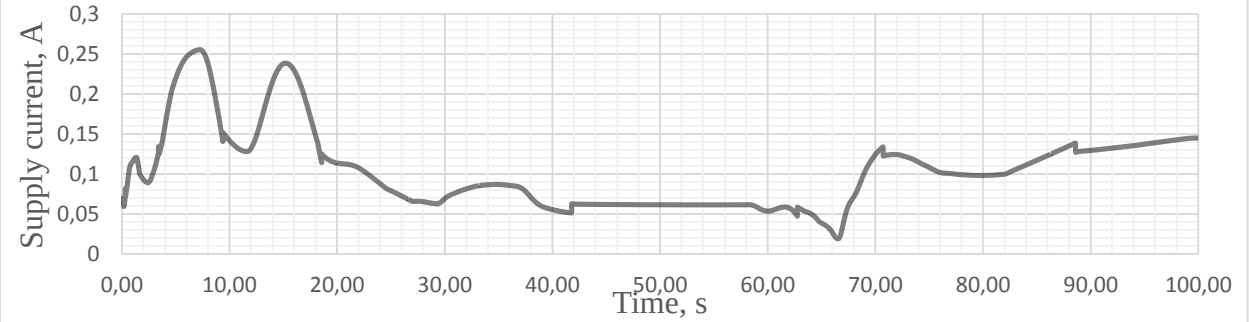

Figure 7 – An example of changing an input variable V5

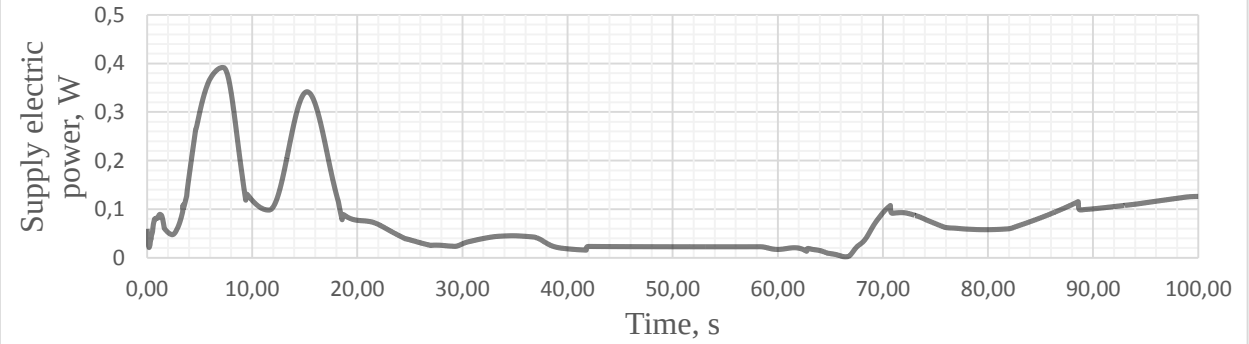

Figure 8 – An example of changing an input variable V6

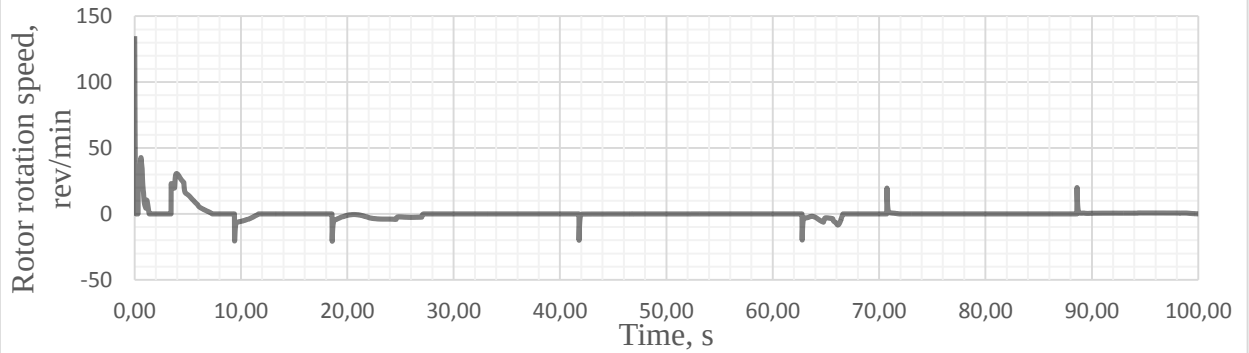

Figure 9– An example of changing an input variable V7

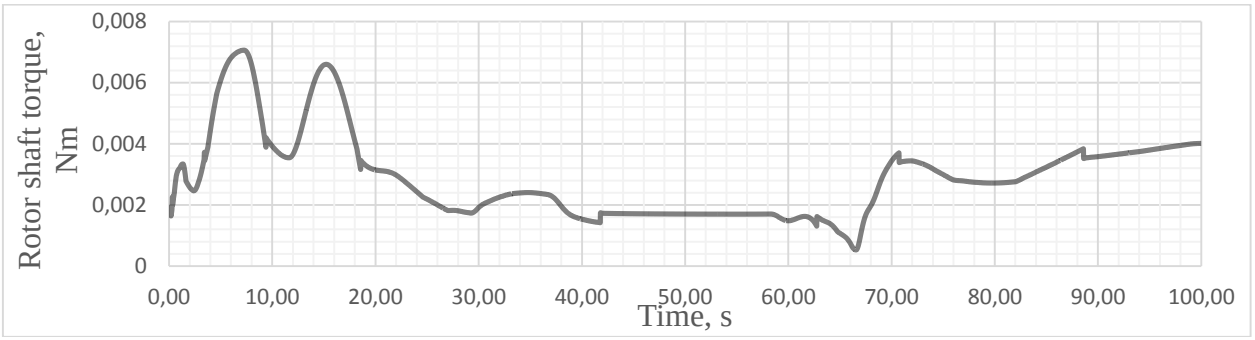

Figure 10 – An example of changing an input variable V8

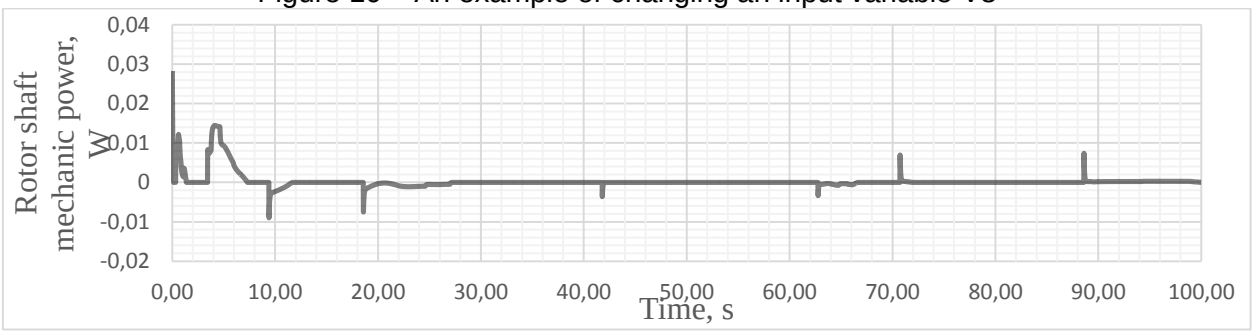

Figure 11 – An example of changing an input variable V9

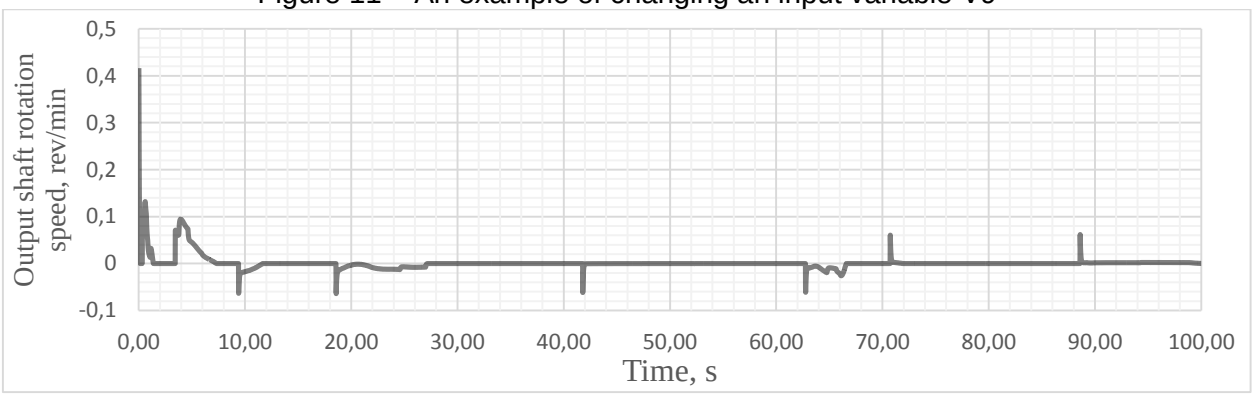

Figure 12 – An example of changing an input variable V10

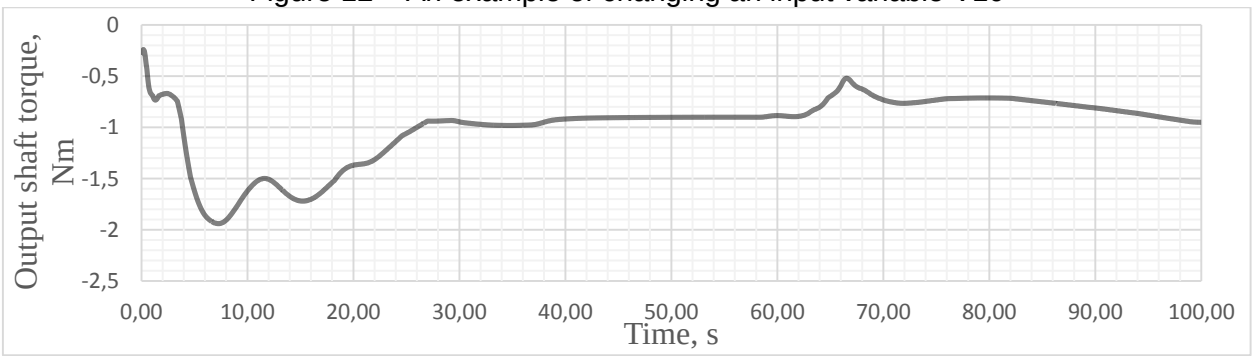

Figure 13 – An example of changing an input variable V11

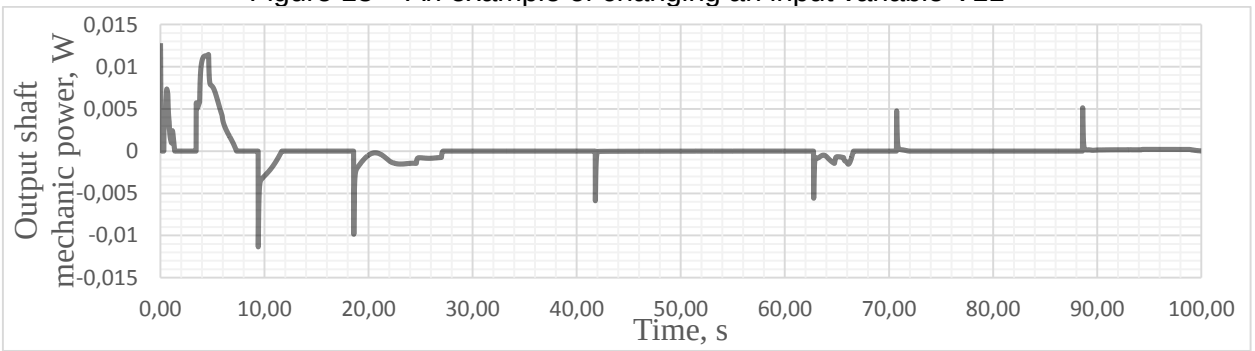

Figure 14 – An example of changing an input variable V12

Each flight cyclogram at a given moment of dry friction Tc (see Table 2) includes 10,000 measurements for each parameter V1-V12. Accordingly, the training set contains 20,000 examples, and the test set contains 60,000 examples. Without using the data processing scheme shown in Figure 1, the accuracy of the neural network with a maximum number of 16 neurons in the hidden layer on the test sample is maximum 96.7%. Because Neural network training is not a deterministic algorithm, 50 neural networks were trained, in which from 4 to 16 neurons are used in the hidden layer, the activation functions are hyperbolic tangent (tanh). The parameters of the best 5 neural networks and the obtained accuracy on the test and training samples are presented in Table 4.

Table 4 - Neural networks with input parameters V1-V12 when working out the flight cyclogram

Number of neurons			Classification accuracy	
Input layer	Hidden layer	Output layer	Training sample (%)	Test sample (%)
12	11	2	98,7300	93,96167
12	16	2	99,3800	96,70167
12	12	2	95,0700	92,41167
12	11	2	98,3000	95,02167
12	10	2	99,9800	94,79000

Accuracy refers to the percentage of correctly classified vectors.

Let us reduce the number of features within the framework of the scheme presented in Figure 1. Figure 2 shows the results of applying the feature selection algorithms described in Section 3.

Parameters related by regression dependence (Stage 1)

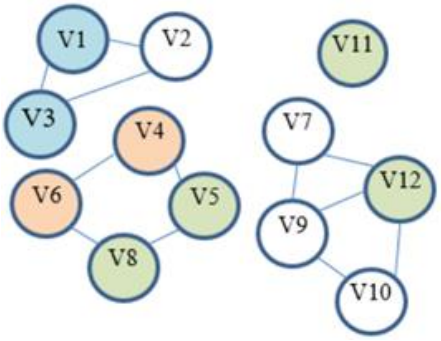

Chi-square test result (Stage 2)

Название переменной	Важность параметра (по хи-квадрат тесту)	p-level
V2	41807,30	0,000000
V3	41807,30	0,000000
V1	40590,56	0,000000
V5	19452,68	0,000000
V8	19452,68	0,000000
V4	19272,22	0,000000
V6	14806,20	0,000000
V9	1811,61	0,000000
V7	115,80	0,000000
V10	115,80	0,000000
V12	26,56	0,005362
V11	10,22	0,009165

Figure 15 – Selection (filtering) of features for training a neural network

Figure 15 shows that the EMA parameters form 4 groups of interconnected elements. In each selected group, as the inputs of the neural network, we select one parameter that is of the greatest importance (informativeness) according to the chi-square test. Accordingly, the parameters V2, V5, V9, V11 are considered as potential inputs of the neural network. The results of optimization of a subset of parameters by the exhaustive search method show that the maximum accuracy on the training and test samples is achieved only when all 4 parameters are used. In total, 50 neural networks (with input parameters V2, V5, V9, V11) were trained, in which from 4 to 16 neurons are used in the hidden layer, the hyperbolic tangent is used as the activation functions of neurons in the hidden layer. The parameters of the best 5 neural networks and the obtained accuracy on the test and training samples are presented in Table 5.

Table 5. Neural networks with input parameters V2, V5, V9, V11 when working out the flight cyclogram

Number of neurons			Classification accuracy	
Input layer	Hidden layer	Output layer	Training sample (%)	Test sample (%)
4	14	2	99,98500	98,01000
4	15	2	99,04500	95,14333
4	11	2	96,68500	95,40500
4	16	2	99,79000	96,70667
4	11	2	96,68000	94,00167

Thus, with a decrease in the number of input parameters, it was possible to slightly increase the accuracy and reduce the number of neurons. It should also be noted that the learning rate of neural networks has significantly increased. Figure 16 shows the result of applying a neural network, which showed an accuracy of 98.01%, on a test sample when working out the flight sequence for the dry friction torque Tc = 0.225 (training sample, class 1 - good condition).

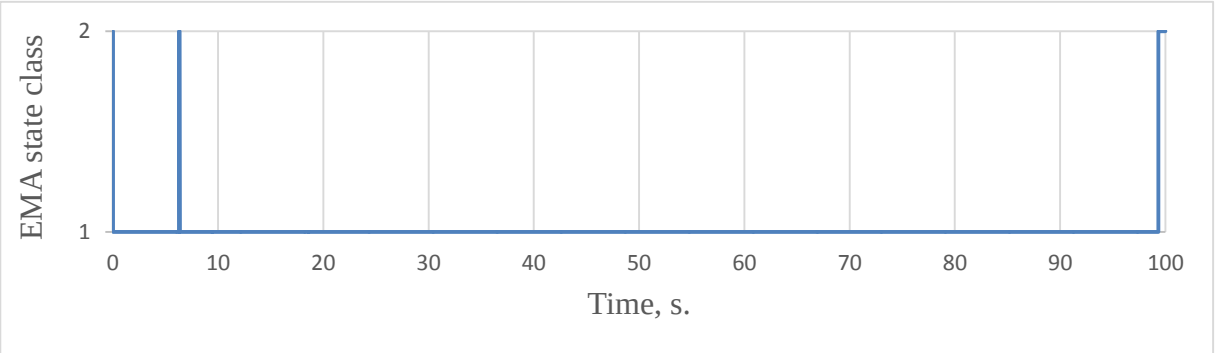

Figure 16 – The result of using a neural network when working out the flight cyclogram (training sample, class 1 - healthy condition)

Figure 17 shows the result of using the neural network when working out the flight cyclogram for the dry friction moment Tc = 0.375 (test sample, class 1 - healthy condition). The worst case is shown due to the use of the cutoff value from the Tc range.

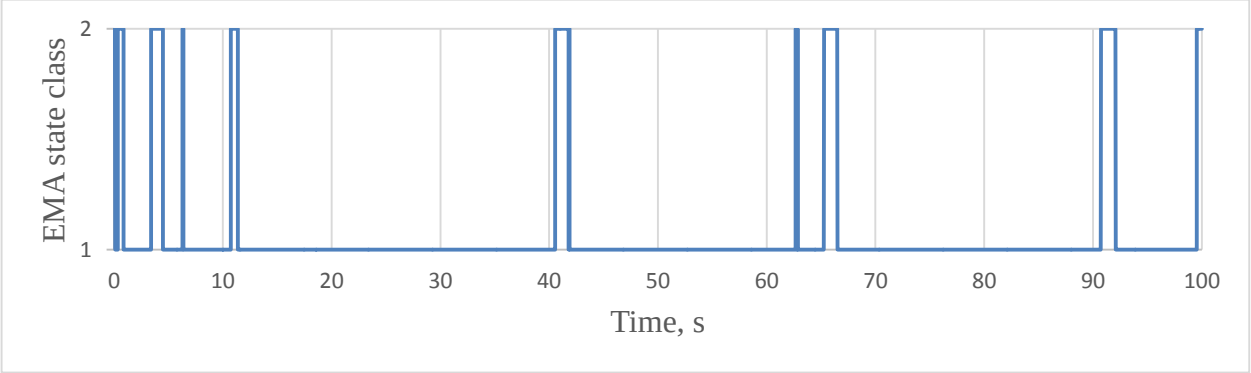

Figure 17 – The result of using a neural network when working out the flight cyclogram (test sample, class 1 - healthy condition)

Figures 16 and 17 show that when determining the EMA working state on the test sample, in comparison with the training sample, there are more time ranges in which the neural network erroneously determines the class of the EMA technical state - the healthy condition is taken as faulty. Figure 18 shows the result of using the neural network when working out the flight sequence for the dry friction moment Tc = 1.025 (training sample, class 2 - faulty state).

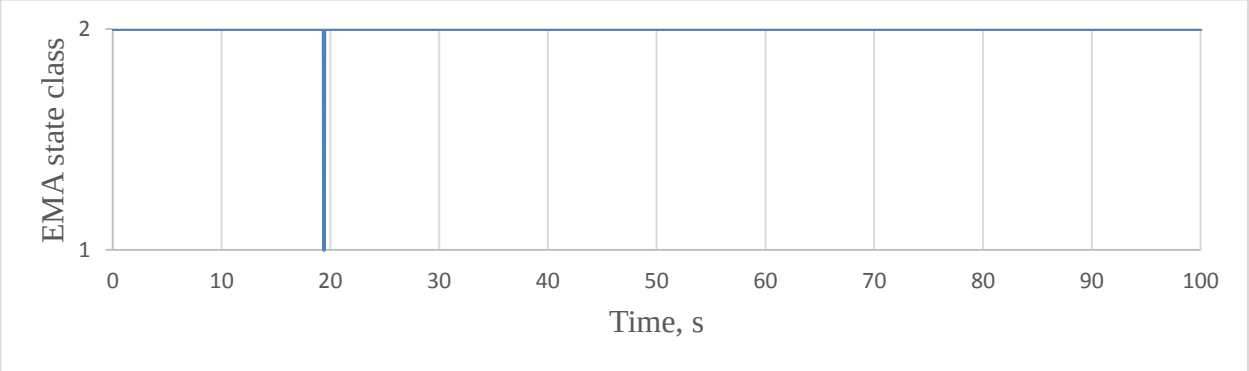

Figure 18 – The result of using a neural network when working out the flight cyclogram (training sample, class 2 - faulty state)

Figure 19 shows the result of using the neural network when working out the flight cyclogram for Tc = 0.875 (training sample, class 2 - faulty state). It also shows the worst result due to the use of the cutoff value from the Tc range.

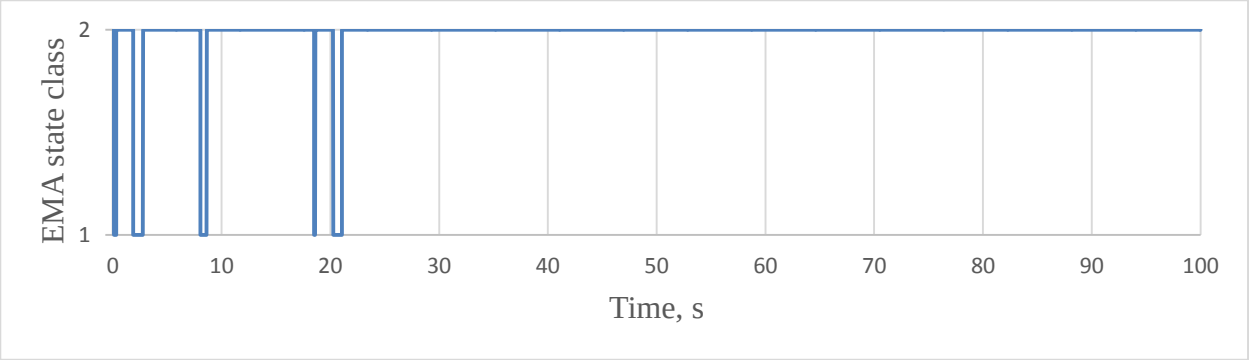

Figure 19 – The result of using a neural network when working out the flight cyclogram (test sample, class 2 - faulty state)

Figures 18 and 19 show that when determining the EMA faulty state on the training sample, in comparison with the test sample, there are also more time ranges, in which the neural network erroneously determines the class of the EMA technical state - the faulty state is taken as good.

6. Conclusion

As carried out studies have shown the effectiveness of data mining methods for determining the UAV control surface EMA technical state based on dissipative losses in a mechanical gearb. Using the developed scheme for data analysis on the example of the results of simulation the operating cyclogram of the EMA during UAV takeoff, the following results were achieved: the number of parameters was reduced from 13 to 4, the number of neurons in the hidden layer of the neural network was reduced, while the accuracy of recognizing the EMA technical state on the test sample was slightly increased (from 96.70167 to 98.01).

Further development of the work is expected in the direction of simulation on a larger number of flight modes and expanding the EMA degradation parameters list, functioning in various technical states. For this, it is supposed to detail the gearbox energy losses model - the use of modeling friction in a two-mass system (Karnop's model), which allows, in addition to changing the friction losses parameters, to control such a degradation parameter as mechanical backlash.

7. Contact Author Email Address

mailto: aleksey.skryabin@tsagi.ru

8. Copyright Statement

References

[1] V. Kuvshinov and others. Safety & energy efficiency research on advanced more electrical flight control actuation systems for short/middle range passenger aircraft // More Electric Aircraft Proceedings, 2015, Toulouse, France.

[2] I. Ogoltsov abd others. New developments of electrically powered electrohydraulic and electromechanical actuators for the more electric aircraft // 29th Congress of the International Council of the Aeronautical Sciences, 2014, Saint Petersburg, Russia.

[3] J.-C. Derrien. Electromechanical actuator (EMA) advanced technologies for flight controls // 28th International Congress of the Aeronautical Sciences, 2012, Brisbane, Australia.

[4] E. Glison, J.D. Kopp, D. Manzanares, Moog next generation control and actuation in R3ASC Conference Proceedings, Toulouse. 2014, pp. 43 54.

[5] Balaban E., Bansal P., Stoelting P. A diagnostic approach for electro-mechanical actuators in aerospace systems. IEEE Aerospace conference. Big Sky. MT. USA. 2009. paper #1345.

[6] Van Der Linden F., Dreyer N., Dorkel A. EMA Health monitoring : an overview. R3ASC. Toulouse. 2016. p. 21-26.

[7] Todeschi M., Baxerred L. Airbus – health monitoring for the flight control EMAs 2014 status and perspectives. R3ASC. Toulouse. 2014. p. 73 83.

[8] P. E. Greenwood, M. S. Nikulin. A guide to chi-squared testing. — New York: Wiley, 1996.

[9] G.S. Veresnikov,D.E. Goutsevyich, A.V. Skryabin The development of mathematical model for investigating the algorithms of estimation and prediction of UAV electromechanical actuator technical state // IzvestiyaSFedU. Engineering Sciences, 7(209), 2019, Taganrog, pp. 170-181.

[10]R. Kowalski, F. Möller, P. Gallun, A. Bierig Test facility for electro-mechanical actuation systems // Proceedings of the 7th International Workshop on Aircraft Systems Technologies, Hamburg, Germany, 2019, pp. 133-142.

[11]L. Bilyaletdinova, A. Steblinkin Simulation of direct drive electromechanical actuator with ballscrew // Dynamics and Vibroacoustics of Machine (DVM2016) / Procedia Engineering 176 (2017) pp. 85-95.